The petrosal bone and inner ear of *Micromeryx flourensianus* (Artiodactyla, Moschidae) and inferred potential for ruminant phylogenetics

Loïc Costeur

Naturhistorisches Museum Basel, Augustinergasse 2, 4001 Basel, Switzerland,

E-mail: loic.costeur@bs.ch

Abstract

While petrosal bones have a long research history in artiodactyl phylogenetics, the inner ear embedded in this bone has rarely been investigated. I describe here a set of petrosals and the associated inner ears of the Middle Miocene moschid *Micromeryx flourensianus* from the German locality Steinheim and compare them to the extant musk deer *Moschus moschiferus* (Moschidae), the four-horned antelope *Tetracerus quadricornis* (Bovidae) and the white-tailed deer *Odocoileus virginianus* (Cervidae). Inner ears were reconstructed using high resolution x-ray computed tomography scans. In phylogenenetic reconstructions built on morphological and molecular data, Moschidae has variously been shown to be a sister taxon to Bovidae or Cervidae. Its position hasn't reached a consensus yet. Studying the inner ear morphology adds new morphological characters that will help resolving this question. *Micromeryx flourensianus* is an abundant fossil moschid and I show indeed that its petrosal bone and inner ear share several similarities with that of the extant musk deer such as a ventral basicapsular groove, a well-developed anterior process of the tegmen tympani, or a fossa for the tensor tympani muscle in the musk-deer that may well have evolved from a *Micromeryx*-like condition. Inner ears share a thick basal cochlear whorl, a bulky vestibule, or a short and thick cochlear aqueduct. This shows that inner ears have a high potential for taxonomy and phylogenetics. Including the inner ear of a fossil skull of *Micromeryx flourensianus* also from Steinheim, four inner ears are described here and give insights into the morphological variability of this structure at an intraspecific level as well as into the post-natal ontogenetic changes that occur. This contribution is a first step towards a comprehensive understanding of the evolution of the ruminant inner ear.

Key words: Ruminantia, Moschidae, Cervidae, Bovidae, bony labyrinth, computed tomography, phylogeny, morphology, Middle Miocene.

---

1. Introduction

The petrosal bone of mammals has long been a source of phylogenetically relevant morphological information. Petrosal characters have brought complementary information that helped resolving phylogenetic issues (Spaulding et al. 2009; O'Leary 2010). Studies on the origin of mammal clades in the fossil record have also benefited from the abundance of this often well preserved bone (e.g., Webb & Taylor 1980; Luo & Gingerich 1999). Its compactness makes it one of the most preservable bones of the mammal skeleton and allows it to be exquisitely preserved as a fossil. Recent scientific advances have made it possible not only to study the external morphology of the petrosal bone but also to investigate its internal structures which are the organs of balance and hearing, i.e., the bony labyrinth or inner ear. These long-known structures in extant (Hyrtl 1845; Gray 1907, 1908) or extinct mammals (Hürzeler 1936; Russell 1964, Ladevèze et al. 2008; Theodor 2010; Luo et al. 2011) also yield phylogenetic information but difficulty in accessing this embedded-in-bone information led to its under-usage. Recent studies based on high resolution x-ray computed tomography of petrosal bones indicate how powerful the morphology of the inner ear is to resolve taxonomic, phylogenetic or ecological-palaeoecological questions (Spoor et al. 2002, 2007; Gunz et al. 2012; Alloing-Seguier et al. 2013).

Attempts to use fossil petrosal bones in ruminant or more broadly Artiodactyla research have been carried out successfully (e.g., Webb & Taylor 1980; O'Leary 2010; Orliac 2012) but very few studies focused on the inner ear itself (e.g., Theodor 2010 for *Cainotherium*; Orliac et al. 2012 for the oldest artiodactyl *Diacodexis*).

As far as ruminants are concerned, several main

questions regarding their origin as a clade and the origin and relationships of crown groups still have no answer and are debated (Bibi 2013). Teeth, primarily used in the fossil record because of their abundance, are very convergent structures so that using them to trace back the origin of the living families in the primitive-looking Late Oligocene to Early Miocene ruminants seems virtually impossible. The only up-to-date well-accepted morphological apomorphies of living pecoran families are the presence of cranial appendages that are non-homologous from a family to the other (e.g., ossicones of giraffes, horns of bovids or antlers of cervids). The absence of cranial appendages in moschids has thus always been a problem. The correlated presence of large upper canines in male musk deers, now known as a plesiomorphic character, has led to ascribe many early pecorans to family Moschidae (e.g., Janis & Scott 1987; Gentry et al. 1999), yielding uncertainty to the calibration points of the ruminant phylogenetic tree.

Late Oligocene-Early Miocene hornless ruminants are very well represented in the fossil record, often by complete to sub-complete skulls preserving the ear region. Now that non-destructive methods are applicable, the morphology of their petrosal bone and of their inner ears has been rendered accessible. Since very few is known as to how reliable inner ears, or to a lesser extent petrosal bones, may be in resolving the phylogenetic affinities of a fossil ruminant, it is interesting to investigate these structures in an extinct pecoran that has long been attributed to a family with living representatives. This is the case of *Micromeryx flourensianus*, a Miocene fossil ruminant confidently belonging to the family Moschidae, of which the extant musk deer *Moschus* is the single living genus. *Micromeryx* was until recently not known by skull material. Recent discoveries in Spain revealed the structure of its skull (Sánchez & Morales 2008). New material, long collected in Steinheim (Middle Miocene, Germany; Heizmann & Reiff 2002) but never published, was found in the collections of the Natural History Museum Basel (NMB). A crushed but almost complete skull and three isolated petrosals were found and are described here. This material was scanned under high resolution x-ray computed tomography and the inner ears were digitally reconstructed. I compare this exquisite material to the extant musk deer *Moschus moschiferus* and to two other living ruminants, a capreoline cervid *Odocoileus virginianus* and a bovine bovid *Tetraceros quadricornis*. Moschids have a long research history in phylogenetics but their positioning as sister group to either cervids or bovids has not yet reached a consensus (Hassanin & Douzéry 2003; Hernández Fernández & Vrba 2005; Sánchez et al. 2010; Hassanin et al. 2012; dos Reis et al. 2012; Bibi 2013). This work contributes to this line of research by adding deep time data and by providing the first morphological comparison of the inner ears of several fossil and recent ruminants.

2. Material and Methods

The fossil material analysed in this study comes from the German Middle Miocene locality Steinheim. Its fauna is very well known and is one of the reference faunas for the Middle Miocene of Europe (ca. 14.5 My, Groschopf & Reiff 1969). Almost all the bones of the skeleton of the common moschid *Micromeryx flourensianus* are known from this locality. Although never published, hundreds of specimens of this species are stored in the collections of the Natural History Museum Basel. A crushed skull NMB Sth.833 and three isolated petrosals confidently attributable to *M. flourensianus* (NMB Sth.828a, NMB Sth.865, and NMB Sth. 866) are studied here. Comparative material of extant ruminants from the family Moschidae and from its two closest living families Cervidae and Bovidae is also studied. A petrosal of *Moschus moschiferus* (NMB 4201), a petrosal of the odocoiline cervid *Odocoileus virginianus* (NMB 9872) and a petrosal of the boselaphine bovid *Tetracerus quadricornis* (NMB 10472) constitute the comparative sample. Odocoileini and Boselaphini are here chosen on availability of material. Representatives of the Boselaphini are further interesting because the tribe is considered by some authors one of the most basal in bovids (Hernández Fernández & Vrba 2005 but contra Hassanin et al. 2012).

All the specimens for this work were scanned with high resolution x-ray computed tomography at the Biomaterial Science Center of the University of Basel using a phoenix nanotom® (General Electric Wunstorf, Germany) equipped with a 180 kV / 15 W nanofocus x-ray source. Various scanning resolutions were employed based on specimen sizes, densities and scan measurement time: NMB Sth.833 (skull of *M. flourensianus*) was scanned at a 60 µm resolution; NMB Sth.828a at 30 µm (*M. flourensianus*); NMB Sth.865 (*M. flourensianus*), NMB Sth.866 (*M. flourensianus)*, and NMB 4201 (*Moschus moschiferus*) at 18.5 µm; NMB 10472 at 25 micrometers (*Tetracerus quadricornis*) and NMB 9872 at 20 micrometers (*Odocoileus virginianus*). Raw data are available upon request. 3D reconstructions of the inner ears were achieved using the segmentation editor of software AVIZO® 7.0. Difference in resolution has no impact on the reconstructions of petrosals or on the segmentation of inner ears. All the extant specimens were isolated petrosals taken from adult skulls stored in the collection of the NMB; the fossil skull is that of an adult and the fossil petrosals are also most probably those of adults except NMB Sth.828a (see discussion). Figure 1 shows the position and orientation of a petrosal bone within the braincase. Petrosals illustrated in Figs 2 to 7 are the results of the 3D reconstructions from the DICOM slices showing surface views of the bones. Since the petrosal bone *of Tetracerus quadricornis* was attached inside the skull and has not been segmented, Fig. 7 also shows surface views of the bone and not a 3D reconstruction of the volu-
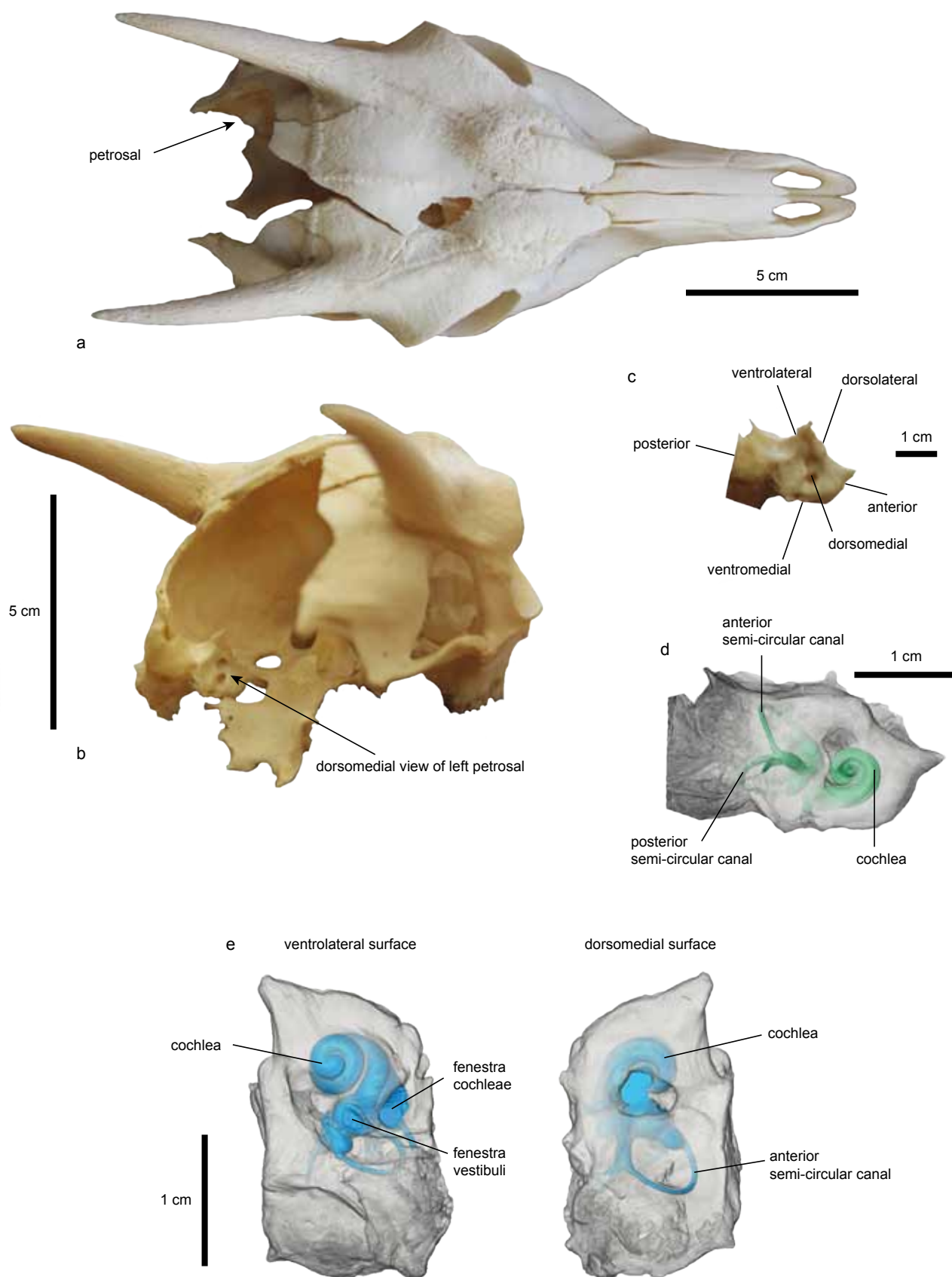
Figure 1: a-d, Position and orientation of the left petrosal bone in NMB 10472 (*Tetracerus quadricornis*). **a**, dorsal view of the skull with position of left petrosal; **b**, latero-occipital view of the skull with dorsomedial surface of left petrosal bone visible; **c**, close-up of left petrosal bone as positioned on the skull showing the orientation of the surfaces; **d**, transparent 3D reconstruction of the petrosal bone with the inner ear inside, the orientation of the petrosal is the same as in c. **e**, two views of the transparent 3D reconstruction of the right petrosal bone NMB Sth.828a (*Micromeryx flourensianus*) showing the orientation of the inner ear within the bone.
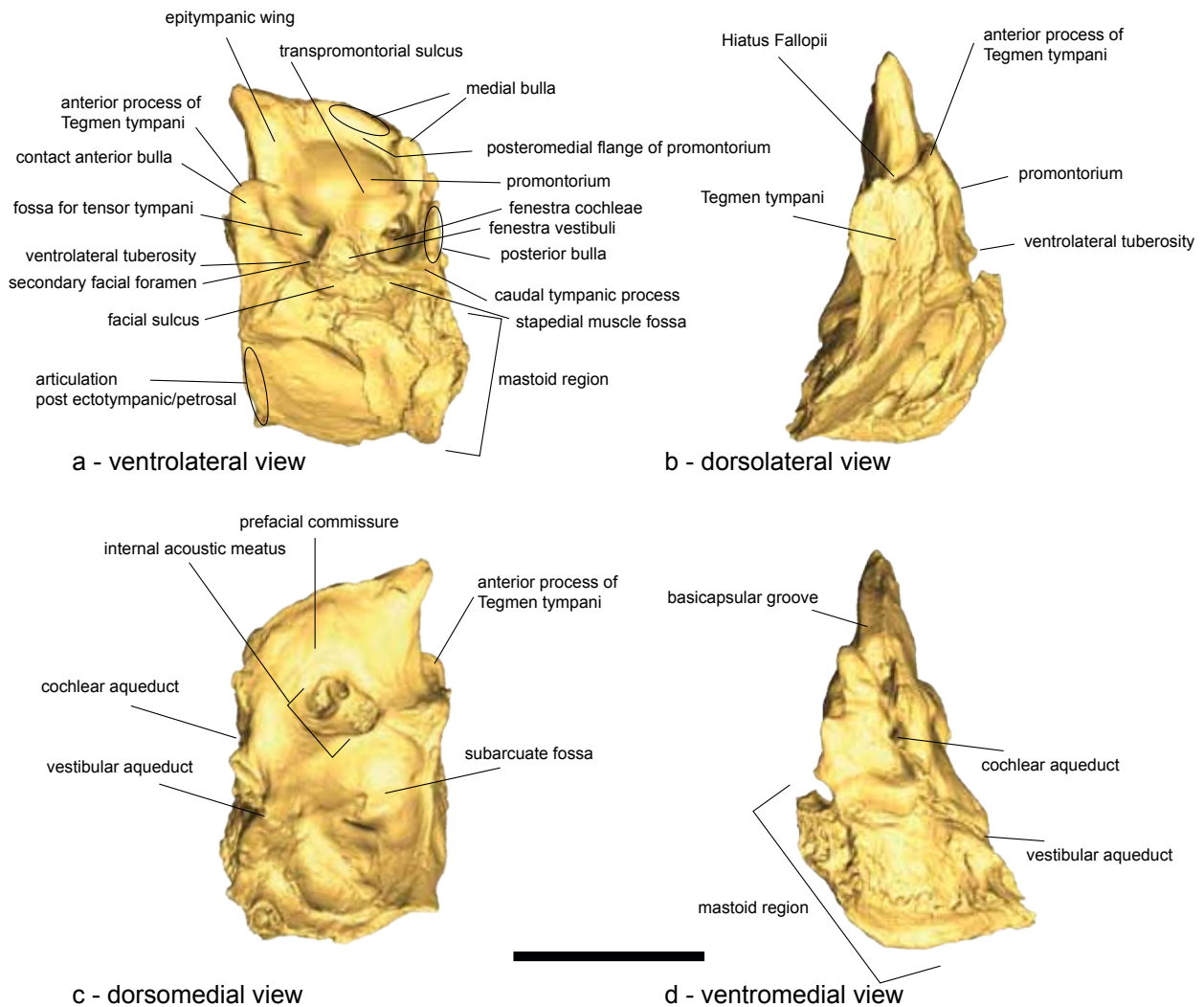
Figure 2: 3D reconstruction of the right petrosal bone NMB Sth.828a of *Micromeryx flourensianus*. **a**, ventrolateral surface; **b**, dorsolateral surface; **c**, dorsomedial surface; **d**, ventromedial surface. Scale bar: 1 cm.

me itself. Some digital processing was necessary to virtually cut parts of skull bones attached to the petrosal that masked parts of it. The mastoid region tightly associated to the skull had to be removed in the process hence its absence, which does however not hamper the description of the relevant parts of the bone for this study.

For comparative purposes images of inner ears are given here with always two of the three semicircular canals aligned in the horizontal and vertical planes. Endolymphatic sacs at the end of vestibular aqueducts were segmented as long as embedded in the petrosal bone; segmentation was stopped when the sac opened on the petrosal surface. The same is true for the cochlear aqueduct.

Inner ear linear and angular measurements were made with the measuring editor in AVIZO® 7.0. Aspect ratio of the cochlea (height divided by width, sensu Ekdale 2013), angles between the planes of the semicircular canals (anterior vs. posterior; ante-

rior vs. lateral; posterior vs. lateral), height and width of the semicircular canals (sensu Ekdale 2013; not given here but briefly discussed) were measured. Degree of coiling of the cochlea was measured on apical views. Measurements follow Ekdale (2013). Nomenclature and orientation for petrosals follow the seminal work of O'Leary (2010). Nomenclature and orientation for inner ears follow Orliac et al. (2012) and Schwarz (2012).

2.1 Abbreviations

aa, asc ampulla; asc, anterior semicircular canal; ca, cochlear aqueduct; cc, common crus; co, cochlea; es, endolymphatic sac; fc, fenestra cochleae; fv, fenestra vestibuli; la, lsc ampulla; lsc, lateral semicircular canal; pa, psc ampulla; pl, primary lamina; psc, posterior semicircular canal; sac, saccule; sl, secondary lamina; ut, utricule; va, vestibular aqueduct.
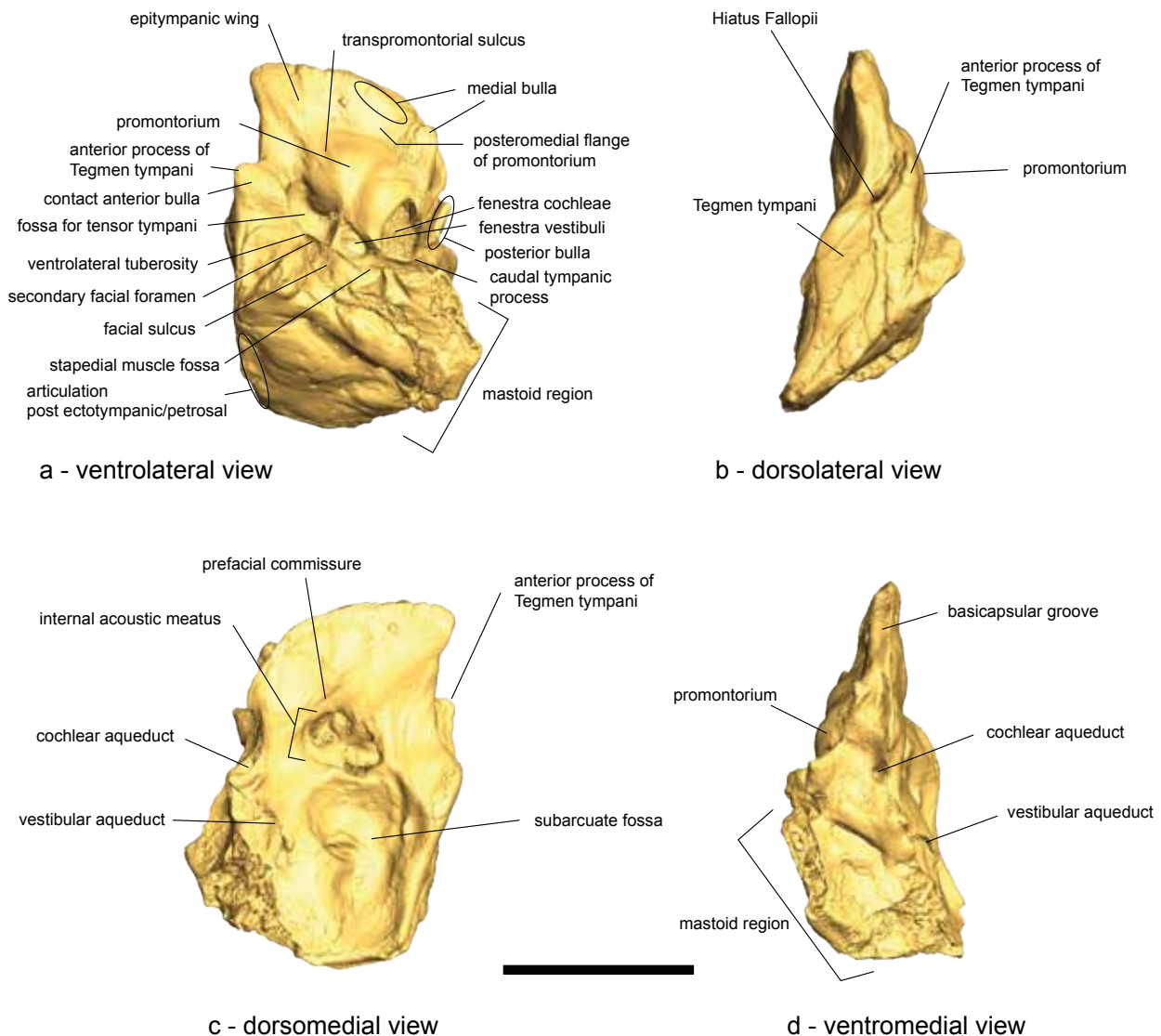
Figure 3: Mirrored 3D reconstruction of the left petrosal bone NMB Sth.865 of *Micromeryx flourensianus*. **a**, ventrolateral surface; **b**; dorsolateral surface; **c**, dorsomedial surface; **d**, ventromedial surface. Scale bar: 1 cm.
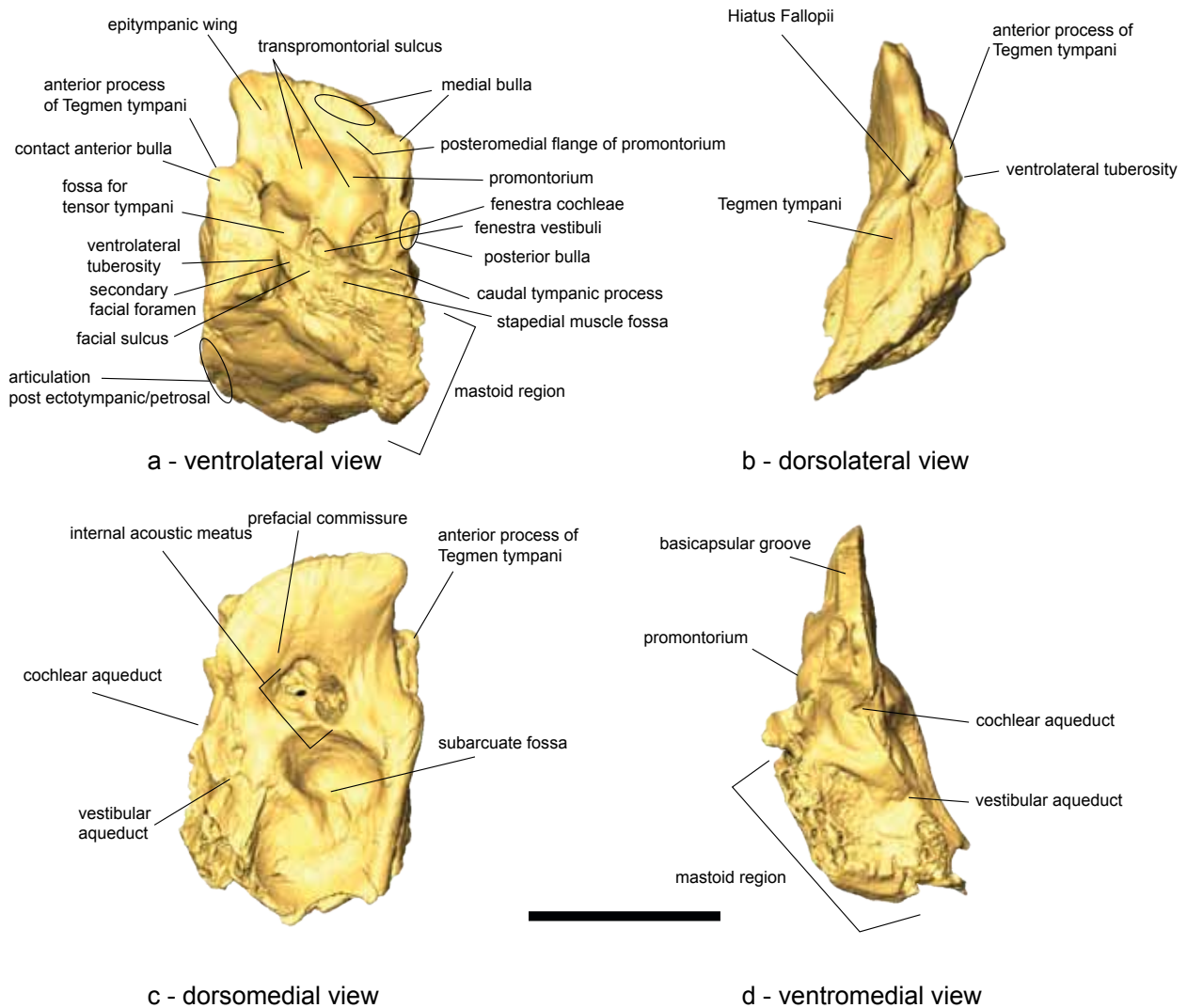
3. Results

3.1 Petrosal bones of *Micromeryx* (Figs 2, 3 and 4) and comparison to *Moschus* (Fig. 5), *Odocoileus* (Fig. 6), *Tetracerus* (Fig. 7).

The three studied petrosal bones of *Micromeryx flourensianus* are remarkably similar (Figs 2, 3 and 4). Preservation state is not identical with a less well-preserved mastoid part on NMB Sth. 865 and NMB Sth.866. The epitympanic wing of both specimens is also slightly less expanded than on NMB Sth.828a because of preservation issues.

Ventrolateral surface (Figs 2a, 3a, 4a, 5a, 6a, 7a). The promontorium on *Micromeryx*'s petrosals has a hemi-ellipsoid shape showing two distinct bulges corresponding to the whorls of the cochlea. The epitympanic wing is large and ends in a pointed apex in *Micromeryx* (Figs 2a, 3a and 4a) and *Tetracerus* (Fig. 7a); it is blunter in *Moschus* (Fig. 5a) and *Odocoileus* (Fig. 6a). All taxa have a more or less expanded posteromedial flange of the promontorium which is continuous with the epitympanic wing. The three isolated fossil petrosals show a transpromontorial groove on the promontorium, which is rather posteriorly placed and has a curved course from a position close to the fenestra cochleae (i.e., round window) towards the apex of the epitympanic wing. By comparison all three extant ruminants have a transpromontorial groove (contra O'Leary 2010 for *Odocoileus* for which it is evidenced here; it is faint but present), which is anteriorly positioned. It also

epitympanic wing
transpromontorial sulcus
anterior process of Tegmen tympani
medial bulla
contact anterior bulla
posteromedial flange of promontorium
fossa for tensor tympani
promontorium
fenestra cochleae
fenestra vestibuli
ventrolateral tuberosity
posterior bulla
secondary facial foramen
caudal tympanic process
stapedial muscle fossa
facial sulcus
articulation post ectotympanic/petrosal
mastoid region

a - ventrolateral view

Hiatus Fallopii
anterior process of Tegmen tympani
ventrolateral tuberosity
Tegmen tympani

b - dorsolateral view

prefacial commissure
internal acoustic meatus
anterior process of Tegmen tympani
cochlear aqueduct
subarcuate fossa
vestibular aqueduct

c - dorsomedial view

basicapsular groove
promontorium
cochlear aqueduct
vestibular aqueduct
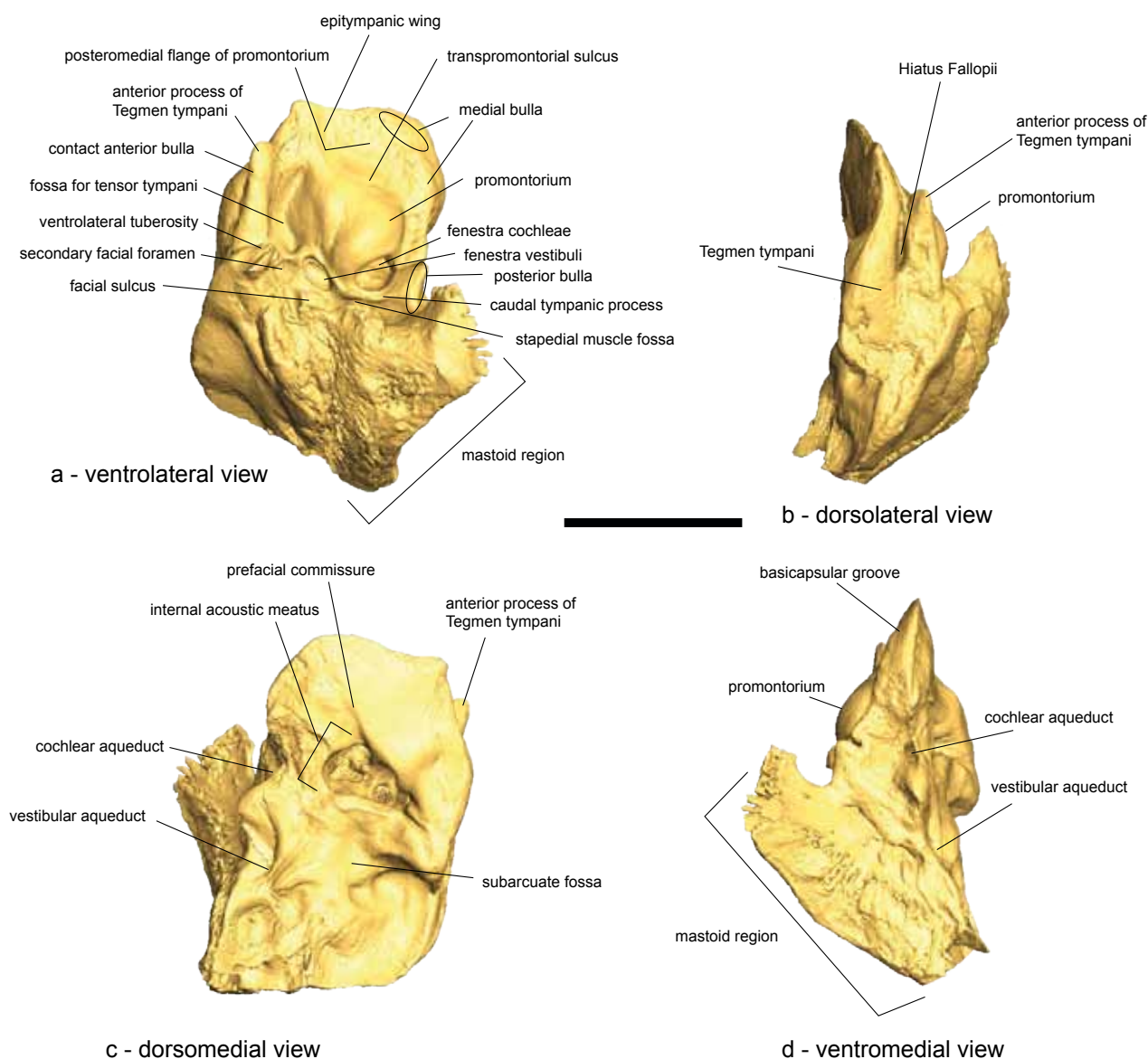mastoid region

d - ventromedial view

Figure 4: 3D reconstruction of the right petrosal bone NMB Sth.866 of *Micromeryx flourensianus*. **a**, ventrolateral surface; **b**, dorsolateral surface; **c**, dorsomedial surface; **d**, ventromedial surface. Scale bar: 1 cm.

shows a curved course but is positioned downslope on the promontorium towards the epitympanic wing. The round opening for the fenestra cochleae is much bigger, at least twice as big as the oval-shaped opening for the fenestra vestibuli (i.e., oval window). As a comparison it is slightly more anteriorly positioned on *Odocoileus* where the fenestra cochleae is also as big as the fenestra vestibuli (Fig. 6a; O'Leary's specimen having a much bigger fenestra cochleae). The fossa for the tensor tympani muscle is not very extended in *Micromeryx*, it has a characteristic slightly curved shape around the posterior part of the promontorium, just below the fenestra vestibuli. Its end next to the latter is quadrangular in shape. It is reminiscent of the more extreme curved situation seen in *Moschus* (Fig. 5a) where it extends longer along the side of the promontorium. It is also slightly deeper in *Micromeryx* than in *Moschus*. The morphology is very different in *Odocoileus* and *Tetracerus* where the fossa has a more rounded to ovoid shape deeply

anchored in the tegmen tympani. This renders the promontorium more elongate whereas it is more bulbous on *Micromeryx* and *Moschus*. The fossa for the head of the malleus, usually situated in the vicinity of the fenestra vestibuli when present like in cetaceans (see O'Leary 2010), always seems to be absent as in other artiodactyls (O'Leary 2010). A secondary facial foramen next to the fenestra vestibuli is always recorded although preservation may obliterate its extent on the fossils. It opens on the facial sulcus. A somewhat ovoid stapedial muscle fossa is visible on NMB Sth.828a (Fig. 2a) and NMB Sth.865 (Fig. 3a). It is less large in *Moschus* and more elongate in *Odocoileus* and *Tetracerus*. A blunt ventrolateral tuberosity is found anteriorly to the external acoustic meatus in *Micromeryx*; its morphology is different in the extant taxa where it can be very flat in *Tetraceus* to high in *Odocoileus* or spike-like in *Moschus*. The tympanic and the petrosal come into contact on the medial border of the pars cochlearis of the petro-
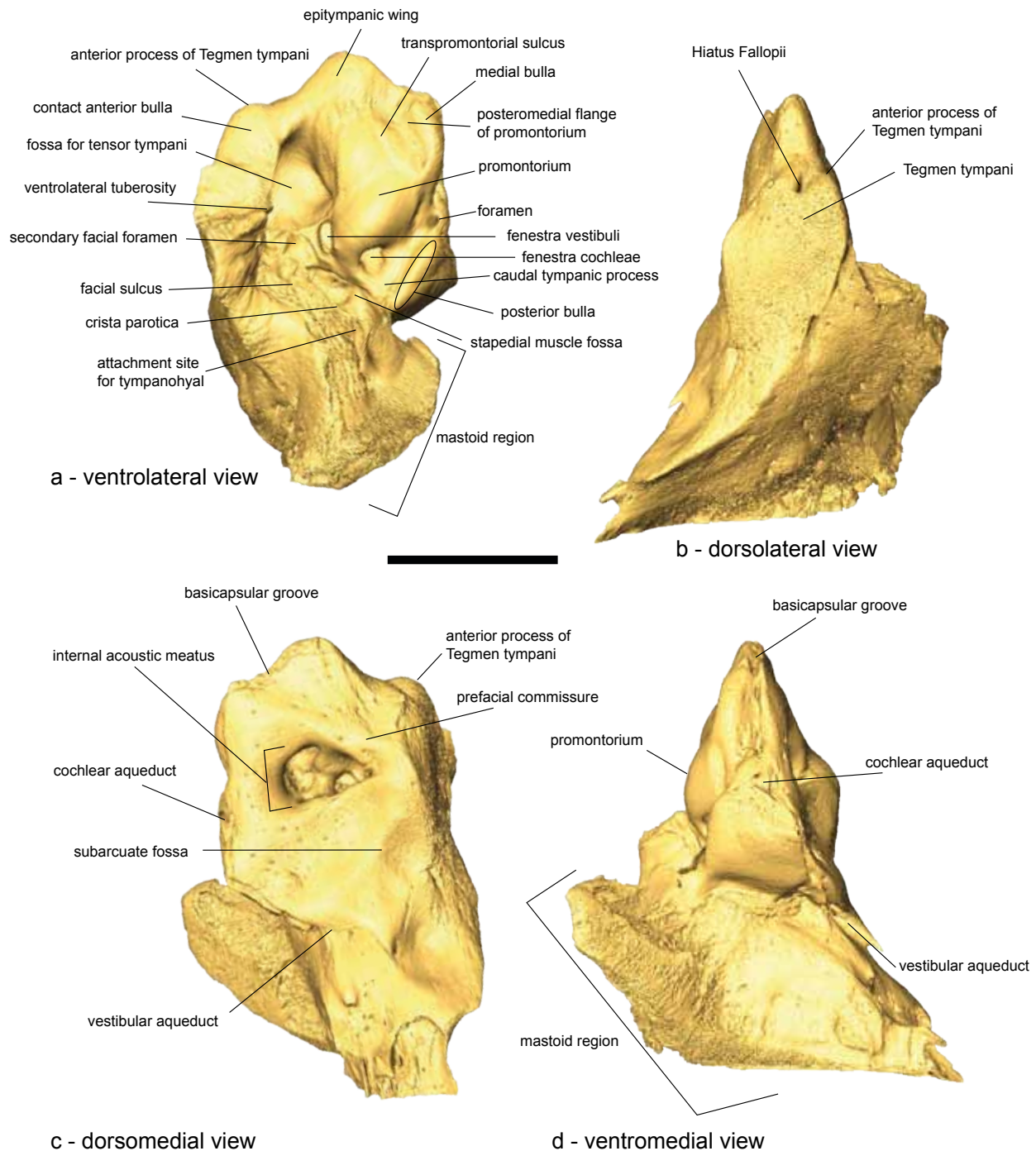
a - ventrolateral view

- epitympanic wing
- posteromedial flange of promontorium
- transpromontorial sulcus
- anterior process of Tegmen tympani
- medial bulla
- contact anterior bulla
- promontorium
- fossa for tensor tympani
- ventrolateral tuberosity
- fenestra cochleae
- secondary facial foramen
- fenestra vestibuli
- posterior bulla
- facial sulcus
- caudal tympanic process
- stapedial muscle fossa
- mastoid region

b - dorsolateral view

- Hiatus Fallopii
- anterior process of Tegmen tympani
- promontorium
- Tegmen tympani

c - dorsomedial view

- prefacial commissure
- internal acoustic meatus
- anterior process of Tegmen tympani
- cochlear aqueduct
- vestibular aqueduct
- subarcuate fossa

d - ventromedial view

- basicapsular groove
- promontorium
- cochlear aqueduct
- vestibular aqueduct
- mastoid region

Figure 5: Mirrored 3D reconstruction of the left petrosal bone NMB 4201 of *Moschus moschiferus*. **a**, ventrolateral surface; **b**; dorsolateral surface; **c**, dorsomedial surface; **d**, ventromedial surface. Scale bar: 1 cm

sal, where the posteromedial flange of the promontorium is extended. Two other articulation surfaces are found below the anterior process of the tegmen tympani for the anterior bulla, and above the caudal tympanic process for the posterior bulla. At this place, the surface is elongate and ellipsoid in shape much like in *Moschus*, whereas it is more elongate in *Odocoileus* and bump-like in *Tetracerus*. The articulation surface with the anterior bulla is longer than in *Moschus* (very fine and elongate and as long as the whole promontorium length) but does not reach the breadth seen in *Tetracerus* and particularly in *Odocoileus*.

Dorsolateral surface (Figs 2b, 3b, 4b, 5b, 6b, 7b). The tegmen tympani is rather small in moschids and moderately inflated in *Odocoileus* and especially in *Tetracerus*. It is smooth and lacks vascular groves

in *Odocoileus* and *Tetracerus* but shows traces of vascular grooves in *Moschus* (Fig. 5b) and in *Micromeryx* (particularly on NMB Sth.865 and NMB Sth. 866, Figs 3b and 4b). The anterior process of the tegmen tympani is longer and pointed in *Micromeryx* and *Moschus*. It is small in *Tetracerus* and *Odocoileus*; in the latter it is almost absent and very blunt. The hiatus Fallopii is always distinct and sits within a deep groove in *Moschus* because of the extended anterior process of the tegmen tympani.

Dorsomedial surface (Figs 2c, 3c, 4c, 5c, 6c, 7c). No prefacial commissure fossa (sensu O'Leary 2010) is visible. *Odocoileus* has a large prefacial commissure running almost perpendicularly across the surface. *Moschus*, NMB Sth. 865 and NMB Sth.866 (Figs 3c and 4c) show a clear and similar-shaped prefacial commissure. The latter is not really visible
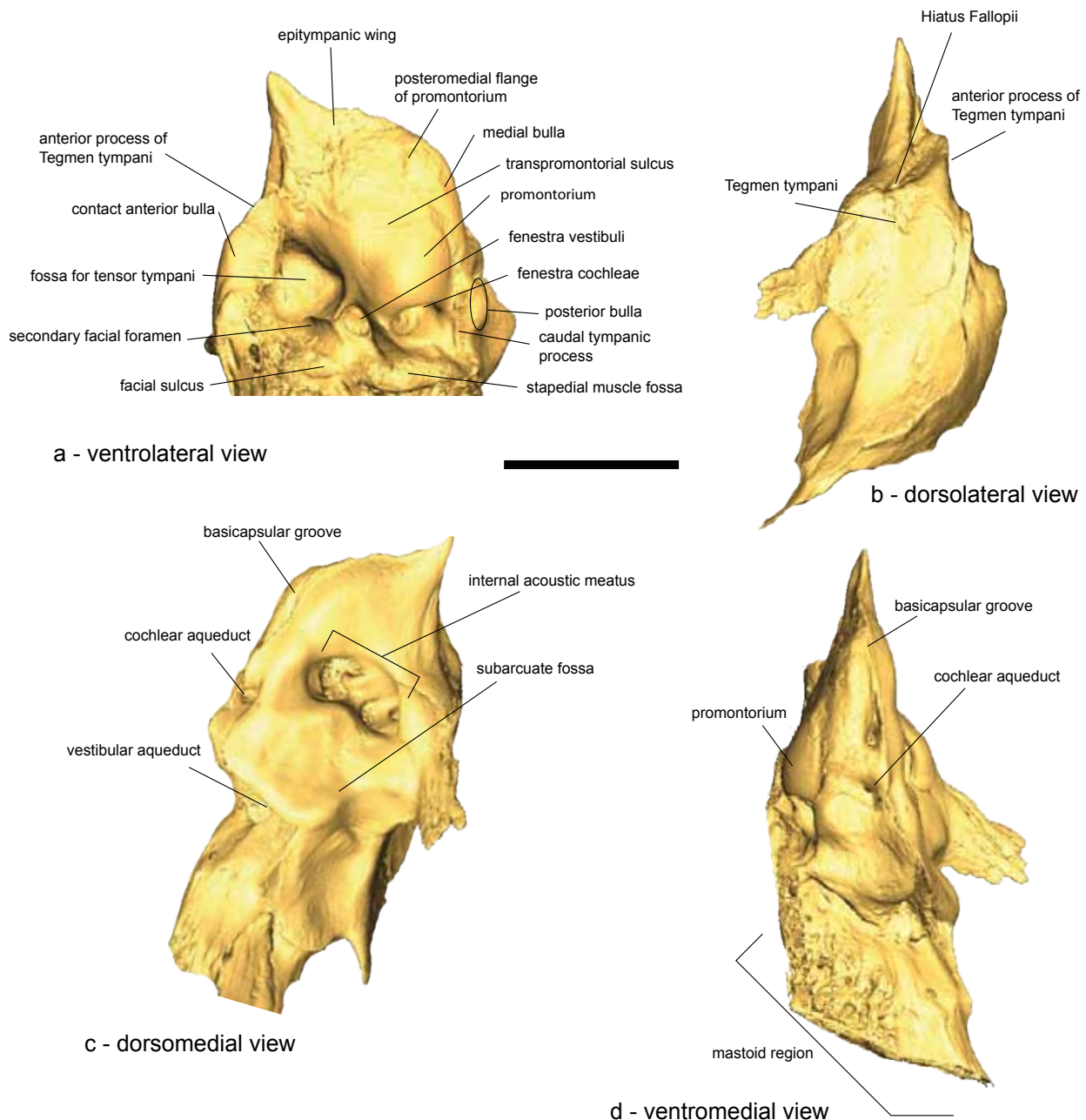
Figure 6: 3D reconstruction of the right petrosal bone NMB 9872 of *Odocoileus virginianus*. **a**, ventrolateral surface; **b**; dorsolateral surface; **c**, dorsomedial surface; **d**, ventromedial surface. Scale bar: 1 cm.

on the other specimens, although a slight and anteriorly placed bar of bone can be evidenced on NMB Sth.828a. The internal acoustic meatus is very variable in shape, being sometimes quite round (NMB Sth. 828a, Fig. 2c and the other fossil petrosals to a lesser extent) to elongate (NMB 10472, Fig. 7c) or triangular (NMB 9872, Fig. 6c). Its shape in *Micromeryx* is most similar to that in *Moschus*. *Odocoileus* and *Tetracerus* have a basicapsular groove running on the ventromedial edge of the petrosal from the tip of

the epitympanic wing down to more or less the level of the internal acoustic meatus i.e., (along the pars cochlearis). This groove is also present in *Moschus* and *Micromeryx*, but is not visible on this view (see below in section ventromedial surface). The basicapsular groove is thus dorsal in *Odocoileus* and *Tetracerus* and ventral in the moschids. The subarcuate fossa is always shallow and wide although its extent and relative depth can slightly change, e.g., NMB Sth.866 (Fig. 4c) has a relatively deeper fossa than

Figure 7: Mirrored 3D reconstruction of the left petrosal bone NMB 10472 of *Tetracerus quadricornis*. **a**, ventrolateral surface, the mastoid region is missing since it had to be virtually cut to help isolate the petrosal bone and make all its surfaces visible; **b**; dorsolateral surface; **c**, dorsomedial surface; **d**, ventromedial surface. Scale bar: 1 cm.

the two other fossil isolated petrosals. The fossa is even shallower in the three extant species described here. The cochlear aqueduct opens posteroventrally to the internal acoustic meatus, its relative size and position can vary from one specimen to the other. The opening for the vestibular aqueduct has a variable position and size too (see also inner ear section below). It is often a large slit situated below the cochlear aqueduct that can run across the surface of the dorsomedial surface (see *Odocoileus* NMB 9872, Fig. 6c). It ends in a bony process (on all specimens studied here) such as already evidenced by O'Leary

(2010) on deers. The mastoid region is always large and wedge-shaped.

Ventromedial surface (Figs 2d, 3d, 4d, 5d, 6d, 7d). The basicapsular groove is visible on this view and is ventrally positioned in all moschids (Figs 2d, 3d, 4d and 5d, facing the promontorium side) while it is dorsally positioned in *Odocoileus* (Fig. 6d) and *Tetracerus* (Fig. 7d). The basicapsular groove is wide and very marked in the three *Micromeryx* specimens while it is more delicate in the extant taxa (although well visible in *Odocoileus*). The groove extends down to the cochlear aqueduct (very clear on *Micromeryx*,

Table 1: Number of turns, degree of coiling and aspect ratio of the cohlea of *Micromeryx flourensianus* (NMB Sth.828a, NMB Sth.833, NMB Sth.865, and NMB Sth.866), *Moschus moschiferus* (NMB 4201), *Tetracerus quadricornis* (NMB 10475) and *Odocoileus virginianus* (NMB 9872). ">2" refers to "slightly more than 2 turns but not reaching 2.5 turns; in these cases, degree of coiling gives a more precise indication.

	NMB Sth.828a	NMB Sth.833	NMB Sth.865	NMB Sth.866	NMB 4201	NMB 10472	NMB 9872
number of turns	>2	2,5	2,5	2,5	>2	2,5	2,5
degree of coiling	755°	900°	900°	900°	785°	900°	900°
aspect ratio	0,685	0,686	0,63	0,667	0,558	0,58	0,536

less visible in *Moschus*). *Odocoileus* has a foramen just above the cochlear aqueduct (see description of ventrolateral surface) where the basicapsular groove seems to end.

3.2 Inner ear of *Micromeryx* (Fig. 8) and comparison to *Moschus*, *Odocoileus*, *Tetracerus* (Fig. 9).

The reconstruction of the inner ear morphology of the *Micromeryx* skull (identified based on dentition morphology) allowed undoubted conspecific identification of the three isolated petrosals studied. All are remarkably similar (except NMB Sth.828a to a certain extent see below). NMB Sth.828a is a fully developed petrosal but the inner ear looks slightly different than the others. These differences will be noted here and most probably find an explanation in a juvenile stage (see discussion).

Figures 8 and 9 illustrate 5 views of the inner ears of *Micromeryx flourensianus* and *Moschus*, *Tetracerus* and *Odocoileus*, respectively. *Micromeryx*'s cochlea completes 2.5 full turns except for NMB Sth.828a which shows slightly more than 2 turns (Table 1). The aspect ratio of the cochlea is high and varies between 0.63 and 0.68 (Table 1). *Moschus* has a little more than two full whorls of the cochlea; *Odocoileus* and *Tetracerus* show 2.5 full turns too. Their aspect ratios are smaller than in *Micromeryx* with 0.56 for *Moschus*, 0.58 for *Tetracerus* and 0.54 for *Odocoileus* (Table 1), classifying the latter in Gray's (1907, 1908) low aspect ratio "flattened cochlea" category (below 0.55). NMB Sth.828a shows a largely overlapping basal whorl, especially towards the fenestra cochleae, a slightly different situation from NMB Sth.865, NMB Sth.866 or NMB Sth.833, where the basal whorl is slightly more detached from the other whorls and less overlapping (Fig. 8 occipital view). All specimens studied here show a secondary lamina, which is long and extends over more than half the length of the basal cochlear whorl in all taxa (Fig. 8 and Fig. 9, medial views). A primary lamina inside the basal cochlear whorl is also visible on all specimens (Fig. 8 and Fig. 9, dorsal views). For *Micromeryx* and *Moschus* all whorls of the cochlea are in close contact, the very end of the basal whorl being sometimes slightly detached. This is not the case for the basal whorl in *Tetracerus* and *Odocoile-*

us, which is slightly more separated from the second one. The basal whorl of the cochlea is thick in *Micromeryx* and *Moschus* (Figs 8 and 9, rostral view) whereas it is less dorso-ventrally expanded in *Tetracerus* and *Odocoileus*. As visible on the ventrolateral surface of the petrosal, the fenestra cochleae is small in the specimen of *Odocoileus*. The fenestra vestibuli is oval-shaped and is more ventrally positioned on the vestibule of *Micromeryx* than on that of the extant species (see *Tetracerus* in particular, Fig. 9, lateral view). The cochlear aqueduct arises at the postero-dorsal edge of the fenestra cochleae. It is oriented posteriorly but takes up various morphologies from small and thick in *Micromeryx* and *Moschus* with a circular cross-section to long and fine in *Odocoileus* with a rather flattened ellipsoid cross-section; *Tetracerus* shows a somewhat intermediate condition.

The vestibule, housing the utricule and saccule between the cochlea and the semi-circular canals, is bulkier in *Micromeryx* and *Moschus* (Fig. 8, lateral view) than in *Tetracerus* and *Odocoileus*, where it looks more detached from the cochlea than on moschids (Figs 8 and 9, medial view). The saccule and utricule are well visible in medial view. The saccule is slightly more inflated on *Micromeryx*, *Odocoileus,* and *Tetracerus* to a lesser extent, than on *Moschus* where both recessi occupy a similar surface. The vestibular aqueduct originates from the vestibule at the base of the common crus, aligned with its midline; it is a variably long structure in *Micromeryx* ending above the dorsalmost extension of the common crus (NMB Sth.833) or below (NMB Sth828a, NMB Sth865 and NMBSth866). The end of the vestibular aqueduct, i.e., the endolymphatic sac, is also variable in size and shape, either being long and narrow (i.e., *Micromeryx* NMB Sth.833) or very short and pouch-like in the other specimens. The vestibular aqueduct is attached to the common crus over most of its course and has a variable curved shape primarily bending to occipital dorsally along its course. The vestibular aqueducts of *Moschus* and *Odocoileus* look much like that of NMB Sth.833; that of *Tetracerus* is detached from the common crus over most of its course and ends in a small but broad pouch.

In *Micromeryx* the asc and lsc are wider than high (sensu Ekdale 2013). The psc is always higher than wide in all specimens. The asc of *Moschus* is higher than wide giving an overall stretched impression

Table 2: Angles (degrees) between the semicircular canals of *Micromeryx flourensianus* (NMB Sth.828a, NMB Sth.833, NMB Sth.865, and NMB Sth.866), *Moschus moschiferus* (NMB 4201), *Tetracerus quadricornis* (NMB 10475) and *Odocoileus virginianus* (NMB 9872). asc, anterior semicircular canal; lsc, lateral semicircular canal; psc, posterior semicircular canal.

	NMB Sth.828a	NMB Sth.833	NMB Sth.865	NMB Sth.866	NMB 4201	NMB 10472	NMB 9872
asc-psc	89°	91°	86°	91°	101°	89.5°	88°
asc-lsc	78°	83°	82°	86°	86°	79°	81°
psc-lsc	90°	89°	87°	90°	91°	89.5°	87°

(Fig. 9, medial view). The same is almost true for *Tetracerus* where both height and width are equal in length. The asc of *Micromeryx* is slightly curved in dorsal view (Fig. 8); this condition is a little more pronounced in *Tetracerus* (Fig. 9, dorsal view) and *Moschus* to a lesser extent. The asc is straighter in dorsal view in *Odocoileus*. The asc constantly shows the greatest dorsal extension of all semicircular canals. The lsc is always straight in lateral view, except for a slight deviation in NMB Sth.865 (Fig. 8, lateral view) and in *Odocoileus* (Fig. 9, lateral view), but it generally does not show any significant deviation from its plane (sensu Ekdale 2013). It always shows some degree of anteroposterior compression. The psc looks similar in *Micromeryx*, *Moschus*, and *Odocoileus* to a lesser extent, but is different in *Tetracerus*. In the latter it shows a characteristic medial flattening towards the ampulla so that it does not look as circular as in the other specimens.

In occipital and rostral views the lsc lies at a level within the ventral and occipital extension of the psc. Its position varies slightly from not exceeding the psc extension (e.g., Fig. 8, NMB Sth.828a or Fig. 9, *Moschus* NMB 4201) to slightly exceeding the psc extension (e.g., Fig. 8, NMB Sth.866 or Fig, 9, *Odocoileus* NMB 9872). Angles between the canal planes were measured and are constant in *Micromeryx*, except for the asc-lsc angle of NMB Sth. 828a which seems slightly smaller than in the three other specimens although no significant difference can be detected (Table 2), a situation that also occurs in *Tetracerus*. *Moschus* stands out with a large asc-psc obtuse angle of 101°. Apart from these exceptions, all other angles in *Micromeryx* and the three extant species are in the same ranges.

The semicircular canals of *Micromeryx* connect to the vestibule through their ampullae at their anterior limbs. The asc and psc ampullae are the most inflated like in *Tetracerus* while the posterior ampulla is the most inflated in *Moschus* and *Tetracerus*. The lsc ampulla lies anteriorly and above the fenestra vestibuli (Figs 8 and 9, lateral and rostral views). As in modern artiodactyls no secondary common crus between the lsc and psc is evidenced. Near the psc

ampulla, the lsc enters the vestibule above the ampulla in *Micromeryx*, *Tetracerus* and particularly in *Moschus* and at the level of the ampulla in *Odocoileus* (Figs 8 and 9, occipital and lateral views). Some variability exists in *Micromeryx* with the posterior limb of the lsc entering the vestibule closer to the psc ampulla in NMB Sth.833 (Fig. 8, occipital view).

The common crus between asc and psc is straight in all specimens but *Tetracerus* where its shape is slightly curved. It is relatively long in *Moschus* and *Tetracerus* and shorter in *Odocoileus* (Fig. 9). It is also rather short in *Micromeryx* (Fig. 8) in comparison to the extant moschid and bovid.

4. Discussion

The comparison of the external and internal anatomy of a set of petrosals including one embedded within a skull of the moschid *Micromeryx flourensianus* from the Middle Miocene German locality Steinheim to the extant moschid *Moschus moschiferus*, the bovid *Tetracerus quadricornis* and the cervid *Odocoileus virginianus* brings to light a number of additional characters that may be used in future phylogenetic analyses. *Micromeryx flourensianus* is a European Miocene taxon for which a moschid affinity is not debated (e.g., Gentry et al. 1999; Vislobokova 2007; Sánchez & Morales 2008; Sánchez et al. 2009, 2010; Aiglstorfer & Costeur 2012). It is the first European moschid with a first occurrence in the early Middle Miocene. It thus represents an interesting case-study to investigate deep time character evolution within family Moschidae.

The petrosal of *Micromeryx flourensianus* shares several characteristics with *Moschus* including a ventrally positioned basicapsular groove while this structure seems to be dorsal in cervids and bovids for which it is known (*Cervus*, *Odocoileus*, *Bos* and *Ovis*, see O'Leary 2010 and *Tetracerus*, *Odocoileus* in this study). The fossa for the tensor tympani muscle bears some resemblance between *Micromeryx* and *Moschus* with a curved and elongate shape, less pronounced in *Micromeryx* and much longer in

Figure 8: Inner ears of *Micromeryx flourensianus* (NMB Sth.828a right, NMB Sth.833 right, NMB Sth.865 left mirrored, and NMB Sth.866 right) in occipital, medial, dorsal, lateral and rostral views. See text for abbreviations (section Material and Methods).

NMB 4201 · NMB 10472 · NMB 9872

occipital · medial · dorsal · lateral · rostral

5 mm
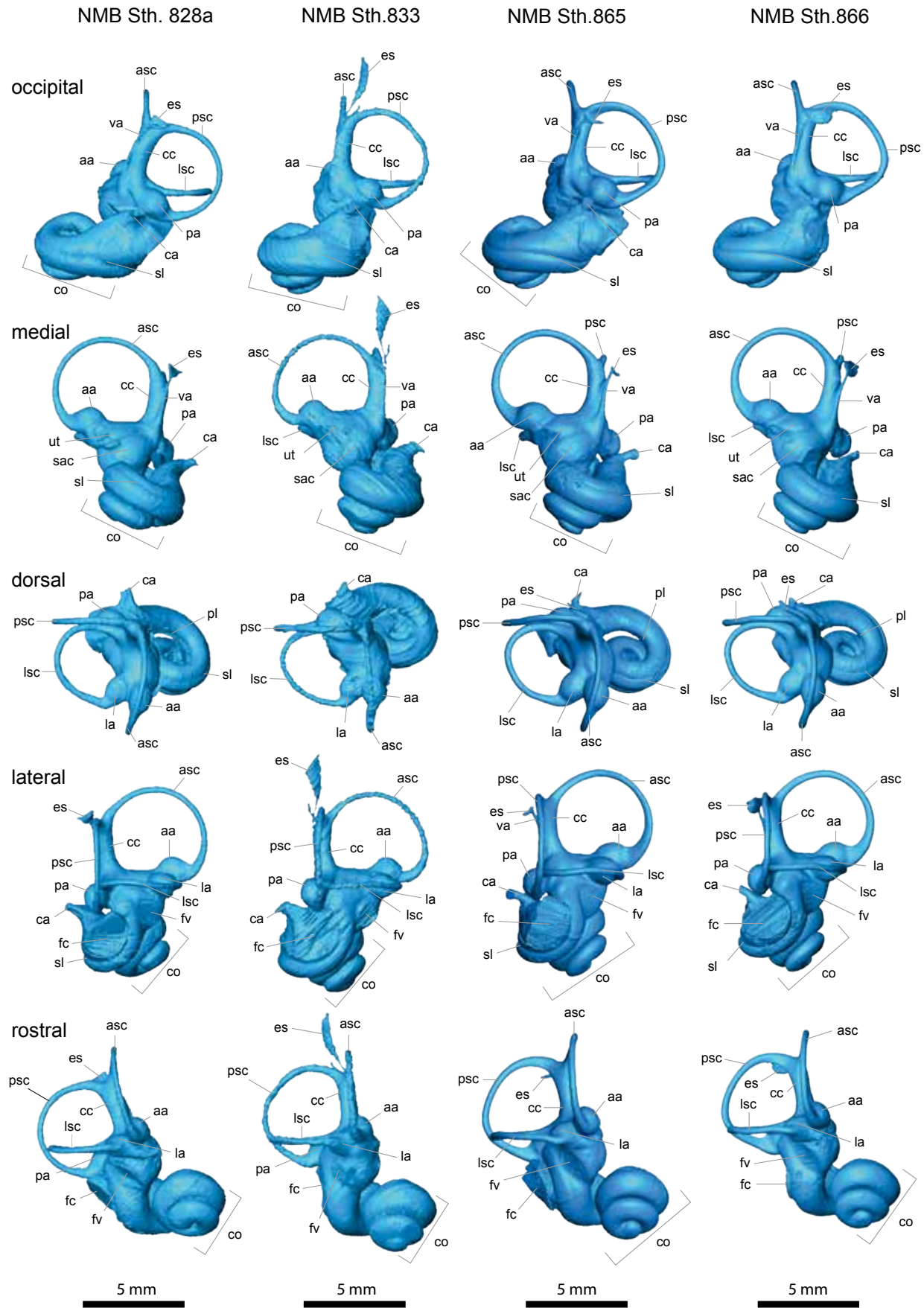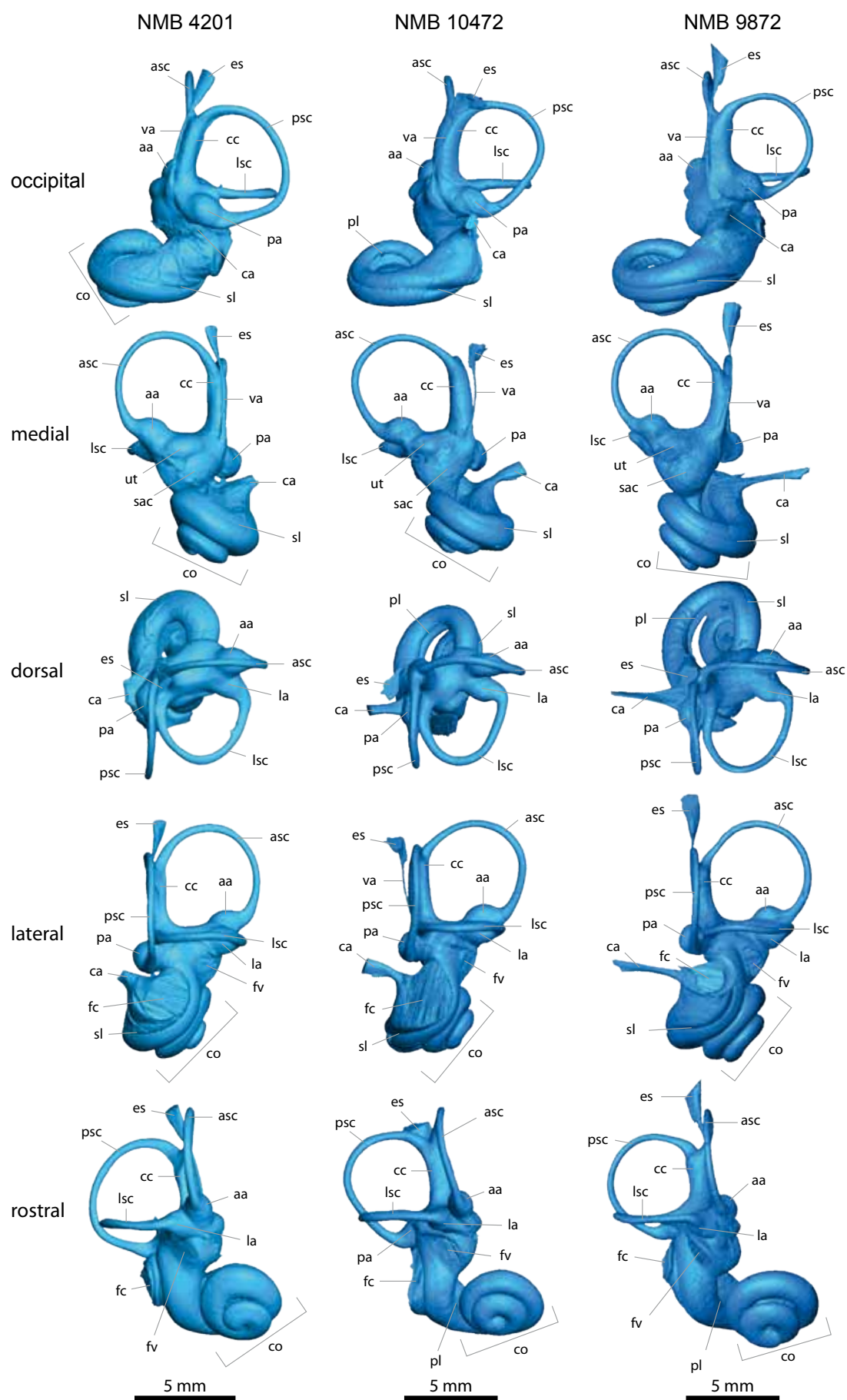
Moschus. The shape of the fossa for the tensor tympani in cervids and bovids is either more quadrangular, or more circular to ovoid. Both moschids have a relatively shallow fossa in comparison to the condition seen in cervids and bovids for which it is known (O'Leary 2010 and this study). Correspondingly, the anterior process of the tegmen tympani is well developed in moschids being elongate and spike-like especially in *Moschus*, responding to the elongate shape of the fossa for the tensor tympani muscle. An evolution of the fossa for tensor tympani muscle and anterior processs of tegmen tympani from a *Micromeryx* condition to a *Moschus* condition would seem reasonable to hypothesize. The condition is very different in living bovids and cervids where the anterior process is smaller and blunt (this study; O'Leary 2010). The prefacial commissure on the dorsomedial surface has a similar shape and position in *Micromeryx* and *Moschus*, but some variability in the fossil taxon also exist with a very flat prefacial commissure in NMB Sth.828a. This structure is broad and long in *Odocoileus* and very flat in *Tetracerus* and is variably developed but always rather faint in other living ruminants (O'Leary 2010). The tegmen tympani on the dorsolateral surface is moderately inflated in cervids and bovids (O'Leary 2010; this study) but seems smaller in moschids. A common feature of *Moschus* and *Micromeryx* would be the presence of vascular grooves on the tegmen tympani, which are absent in *Tetracerus*, *Odocoileus*, *Cervus*, *Bos* or *Ovis* (O'Leary 2010; this study)

Pecoran ruminant inner ears have very rarely been investigated. After the two seminal works of Hyrtl (1845) and Gray (1907, 1908), where only a total of 7 extant pecorans are described, very little information on pecorans inner ears has been published. Also the data presented in these papers are not easily retrievable. Spoor et al. (2007) investigated some pecoran inner ears in an attempt to reconstruct locomotor abilities in terrestrial and marine mammals but they did not illustrate or describe the inner ears themselves. Maier (2013) recently dramatically increased the knowledge of pecoran inner ears by investigating histological serial sections for 17 extant pecorans. His purpose was to identify the entotampanic in late fetal stages, so that adult specimens were not dissected and the 3D morphology was not reconstructed. The 3D morphology of the inner ears of extant pecoran ruminants is thus virtually unknown, and to the best of my knowledge, that of fossil ruminant inner ears too.

The inner ears of *Micromeryx* and *Moschus* share a number of common features. While the number of turns of the cochlea is different, 2.5 in *Micromeryx* (degree of coiling: 900°) and a little more than 2 in *Moschus* (degree of coiling: 785°), the expansion of the vestibule, the tightly coiled cochlear spiral and thick basal whorl, the bulky shape of the cochlear aqueduct, the curved asc (also seen in *Tetracerus*) are shared by the fossil and living moschid. *Moschus* is different from *Micromeryx* in having a higher asc giving a slightly more stretched shape to the inner ear. *Tetracerus* stands out with a less circular psc. *Odocoileus* has a very different, very long and fine cochlear aqueduct and its cochlea is flatter. *Tetracerus* and *Odocoileus* have a basal cochlear whorl which is detached from the other whorls on a third of its length.

NMB Sth.828a looks like the other *Micromeryx* inner ears but has a number of notable differences. They include a smaller angle between the asc and lsc (Table 2), a bulkier cochlea with a more overlapping basal whorl and a lower degree of coiling (755° vs. 900° in the others, Table 1). Observations made on a post-natal ontogenetic series of living *Tragulus kanchil* (Tragulidae; personal observations) indicates that the cochlea is not fully formed in a very young individual. While the petrosal is fully ossified and the inner fully functional at birth in artiodactyls or other mammals (i.e., in primates Jeffery & Spoor 2004), it is not uncommon to see a smaller cochlea in early post-natal stages (i.e., in marsupials Sánchez-Villagra & Schmelzle 2007). Hence, I attribute this lower degree of coiling in NMB Sth.828a to a juvenile stage.

Intraspecific variability evidenced here on the three *Micromeryx* adult inner ears is minimal (very slight differences in angles between the canals, see Table 2, or in canal deviation, see Fig. 8, lateral view of NMB Sth.865). The most variable feature is the length of the vestibular aqueduct and morphology of the endolymphatic sac at its end. Observations made on several inner ears of adult *Tragulus kanchil* (work in progress) confirm this low intraspecific variability. This makes the inner ear a powerful object for phylogenetic reconstructions such as demonstrated in primates (Gunz et al. 2012).

5. Conclusions

This comparison of the petrosal bone of the Middle Miocene moschid *Micromeryx flourensianus* to the extant moschid *Moschus moschiferus* and to a bovid *Tetracerus quadricornis* and a cervid *Odocoileus virginianus* is the first of its kind in ruminants that includes the bony labyrinth.

Several characteristics of the petrosal show large coincidence between the extinct moschid and the living musk-deer (e.g, position of basicapsular

Figure 9: Inner ears of *Moschus moschiferus* (NMB 4201, left mirrored), *Tetracerus quadricornis* (NMB 10475, left mirrored) and *Odocoileus virginianus* (NMB 9872, right) in occipital, medial, dorsal, lateral and rostral views. See text for abbreviations (section Material and Methods).

groove, shape of the fossa for the tensor tympani muscle, shape and extent of the anterior process of the tegmen tympani, or vascular grooves on tegmen tympani). Likewise, the inner ears of *Micromeryx* and *Moschus* share similarities that are not present in the cervid and bovid studied here (e.g., thick basal cochlear whorl, shape of cochlear aqueduct, or bulky vestibule).

These results provide a good basis for future use of ruminant inner ears in phylogenetic analyses. However, before doing so and tackling the question of moschid affinities, ontogenetic studies have to be carried out in order to better understand the development of this structure in ruminants since postnatal changes are known to occur. This is particularly important, since petrosals very quickly ossify in ontogeny, and hence it is not simple to discriminate between fossil isolated juvenile and adult petrosals. Accordingly this has bearings on the systematic ascription of fossil inner ears based on morphological characters, or more importantly on using characters of inner ears in phylogenetic analyses. The same is true for the study of intraspecific variability. First hints suggest it may be minimal in adult specimens and indicate the high potential of inner ears. Future research needs to focus on increased taxonomic, ontogenetic, and intraspecific sampling to identify macro- and micro-evolutionary patterns which might help establishing phylogenetic relationships. Additionally, 3D geometric morphometrics of the inner ears shape, which has recently proven to have a very high discriminative potential (Gunz et al. 2012), have to be considered for ruminants.

Acknowledgements

6. References

Aiglstorfer M, Costeur L. 2012. The Moschidae of Dorn-Dürkheim 1 (Germany). Palaeobiodiversity and Palaeoenvironments 93, 207-215

Alloing-Séguier L, Sánchez-Villagra MR, Lee MSY, Lebrun R. 2013. The bony labyrinth in diprotodontian marsupial mammals: Diversity in Extant and Extinct Forms and Relationships with Size and Phylogeny. Journal of Mammalian Evolution 20(3), 191-198.

Bibi F. 2013. A multi-calibrated mitochondrial phylogeny of extant Bovidae (Artiodactyla, Ruminantia) and the importance of the fossil record to systematics. BMC Evolutionary Biology 13(166), 1-15.

dos Reis M, Inoue J, Hasegawa M, Asher RJ, Donoghue PC, Yang Z. 2012. Phylogenomic datasets provide both precision and accuracy in estimating the timescale of placental mammal phylogeny. Proceedings of the Royal Society B 279, 3491-3500.

Ekdale EG. 2013. Comparative Anatomy of the Bony Labyrinth (Inner Ear) of Placental Mammals. PLoS ONE 8(6), e66624.

Gentry A, Rössner GE, Heizmann EPJ. 1999. Suborder Ruminantia. In: GE Rössner, K Heissig (Eds), The Miocene Land Mammals of Europe. München, Verlag Dr. Friedrich Pfeil, 225-258.

Gray AA. 1907. The labyrinth of animals: including mammals, birds, reptiles and amphibians, Volume 1. London, J. and A. Churchill, 98 pp.

Gray AA. 1908. The labyrinth of animals: including mammals, birds, reptiles and amphibians, Volume 2. London, J. and A. Churchill, 252 pp.

Groschopf P, Reiff W. 1969. The Steinheim basin - a comparison with the Ries. Geologica Bavarica 61, 400–412.

Gunz P, Ramsier M, Kuhrig M, Hublin, J-J, Spoor F. 2012. The mammalian bony labyrinth reconsidered, introducing a comprehensive geometric morphometric approach. Journal of Anatomy 220, 529-543.

Hassanin A, Douzéry EJ. 2003. Molecular and morphological phylogenies of Ruminantia and the alternative position of the Moschidae. Systematic Biology 52(2), 206-228.

Hassanin A, Delsuc F, Ropiquet A, Hammere C, Jansen van Vuuren B, Matthee C, Ruiz-Garcia M, Catzeflis F, Areskoug V, Thanh Nguyen T, Couloux A. 2012. Pattern and timing of diversification of Cetartiodactyla (Mammalia, Laurasiatheria), as revealed by a comprehensive analysis of mitochondrial genomes. Comptes Rendus Biologies 335, 32-50.

Heizmann EPJ, Reiff W. 2002. Der Steinheimer Meteorkrater. München, Verlag Dr. Friedrich Pfeil, 160 p.

Hernández Fernández M, Vrba ES. 2005. A complete estimate of the phylogenetic relationships in Ruminantia: a dated species-level supertree of the extant ruminants. Biological Review 80, 269-302.

Hürzeler J. 1936. Osteologie und Odontologie der Caenotheriden. Schweizerische Paläontologische Abhandlungen 58, 89 p.

Hyrtl J. 1845. Vergleichende-anatomische Untersuchungen über das innere Gehörorgan des Menschen und der Säugethiere. Prague, Verlag Friedrich Ehrlich, 139 pp.

Janis CM, Scott KM. 1987. The interrelationships of higher ruminant families with special emphasis on the members of the Cervoidea. American Museum Novitates 2893, 1-85.

Jeffery N, Spoor F. 2004. Prenatal growth and development of the modern human labyrinth. Journal of Anatomy 204, 71-92.

Ladevèze S, Asher RJ, Sánchez-Villagra MR 2008. Petrosal anatomy in the fossil mammal Necrolestes: evidence for metatherian affinities and comparisons with the extant marsupial mole. Journal of Anatomy 213, 686-697.

Luo Z-X, Gingerich PD. 1999. Terrestrial mesonychia to aquatic cetacea: transformation of the basicranium and evolution of hearing in whales. University of Michigan papers on Palaeontology 31, 1-98.

Luo Z-X., Ruf I, Schultz JA, Martin T. 2011. Fossil evidence on evolution of inner ear cochlea in Jurassic mammals. Proceedings of the Royal Society London, B 278, 28-34

Maier W. 2013. The Entotympanic in Late Fetal Artiodactyla (Mammalia). Journal of Morphology 275, 926-939.

O'Leary MA. 2010. An anatomical and phylogenetic study of the osteology of the petrosal of extant and extinct artiodactylans (Mammalia) and relatives. Bulletin of the American Museum of Natural History 335, 1-206.

Orliac M. 2012. The petrosal bone of extinct Suoidea (Mammalia, Artiodactyla). Journal of Systematic Palaeontology 11(8),

925-945.

Orliac M, Benoit J, O'Leary MA. 2012. The inner ear of *Diacodexis*, the oldest artiodactyl mammal. Journal of Anatomy 221(5), 417-426.

Russell DE. 1964. Les mammifères paléocènes d'Europe. Mémoires du Museum National d'Histoire Naturelle 13, 324 p.

Sánchez IM, Morales J. 2008. *Micromeryx azanzae* sp. nov. (Ruminantia: Moschidae) from the middle-upper Miocene of Spain, and the first description of the cranium of *Micromeryx*. Journal of Vertebrate Paleontology 28, 873-885.

Sánchez IM, Soledad Domingo M, Morales J. 2009. New data on the Moschidae (Mammalia, Ruminantia) from the Upper Miocene of Spain (MN10-MN11). Journal of Vertebrate Paleontology 29(2), 567-575.

Sánchez IM, Soledad Domingo M, Morales J. 2010. The genus *Hispanomeryx* (Mammalia, Ruminantia, Moschidae) and its bearing on musk deer phylogeny and systematics. Palaeontology 53(5), 1023-1047.

Sánchez-Villagra MR, Schmelzle T. 2007. Anatomy and development of the bony inner ear in the wooly opossum, Caluromys philander (Didelphimorphia, Marsupiala). Mastozoología Neotropical 14(1), 53-60.

Schwarz C. 2012. Phylogenetische und funktionsmorphologische Untersuchungen der Ohrregion bei Sciuromorpha (Rodentia, Mammalia). Ph.D. Thesis, Rheinischen Friedrich-Wilhelms-Universität Bonn, Germany, 350 p.

Spaulding M, O'Leary MA, Gatesy J. 2009. Relationships of Cetacea (Artiodactyla) among mammals increased taxon sampling alters interpretations of key fossils and character evolution. PLoS One 4(9), e7062.

Spoor F, Bajpal S, Hussaim ST, Kumar K, Thewissen JGM. 2002. Vestibular evidence for the evolution of aquatic behaviour in early cetaceans. Nature 417, 163–166.

Spoor F, Garland T, Krovitz G, Ryan TM, Silcox, MT., Walker A. 2007. The primate semicircular canal system and locomotion. Proceedings of the National Academy of Sciences USA 104, 10808-10812.

Theodor JM. 2010. Micro-computed tomographic scanning of the ear region of *Cainotherium*: character analysis and implications. Journal of Vertebrate Paleontology 30(1), 236-243.

Vislobokova I. 2007. New Data on Late Miocene Mammals of Kohfidisch, Austria. Paleontological Journal 41(4), 451-460.

Webb SD, Taylor BE. 1980. The phylogeny of hornless ruminants and a description of the cranium of *Archaeomeryx*. Bulletin of the American Museum of Natural History 167(article 3), 119-157.